

Article

Not peer-reviewed version

Silymarin Alleviates Oxidative Stress and Inflammation Induced by UV and Air Pollution in Human Epidermis and Activates β -Endorphin Release through Cannabinoid Receptor Type 2

[Cloé Boira](#)*, Emilie Chapuis, [Amandine Scandolera](#), [Romain Reynaud](#)

Posted Date: 24 December 2023

doi: 10.20944/preprints202312.1689.v1

Keywords: UVA; UVB; pollutants; NQO1; filaggrin; keratin 16; interleukin 6



Preprints.org is a free multidiscipline platform providing preprint service that is dedicated to making early versions of research outputs permanently available and citable. Preprints posted at Preprints.org appear in Web of Science, Crossref, Google Scholar, Scilit, Europe PMC.

Copyright: This is an open access article distributed under the Creative Commons Attribution License which permits unrestricted use, distribution, and reproduction in any medium, provided the original work is properly cited.

Article

Silymarin Alleviates Oxidative Stress and Inflammation Induced by UV and Air Pollution in Human Epidermis and Activates β -Endorphin Release through Cannabinoid Receptor Type 2

Cloé Boira ^{1,*}, Emilie Chapuis ¹, Amandine Scandolera ¹ and Romain Reynaud ²

¹ Givaudan Active Beauty, 51110 Pomacle, France

² Givaudan Active Beauty, 31400 Toulouse, France

* Correspondence: cloe.boira@givaudan.com

Abstract: Background: Skin is exposed to ultraviolet radiation (UV) and air pollution and recent works demonstrated these factors have additive effects in the disturbance of skin homeostasis. Nuclear factor erythroid 2-related factor 2 (Nrf2) and aryl hydrocarbon receptor (AHR) appears appropriate targets in the management of combined environmental stressors. The protective effects of Silymarin (SM), an antioxidant and anti-inflammatory complex of flavonoids, were evaluated. Methods: Reactive oxygen species (ROS) and interleukin 1-alpha (IL-1a) were quantified in UV+urban dust stressed reconstructed human epidermis (RHE) treated with SM. Gene expression study was conducted on targets related to AHR and Nrf2. SM agonistic activity on cannabinoid receptor type 2 (CB2R) was evaluated on mast cells. Clinical study quantified the performance of SM and cannabidiol (CBD), in skin exposed to solar radiation and air pollution. Results: SM decreased morphological alterations, ROS and IL-1a in UV+urban dust stressed RHE. AHR and Nrf2 related genes were upregulated that control antioxidant effector and barrier function. Interleukin 8 gene expression was decreased. Clinical study confirmed SM to improve homogeneity and perceived well-being of urban skins exposed to UV, outperforming CBD. SM activated CB2R and release of β -endorphin from mast cells. Conclusions: SM provides protection of skin from oxidative stress and inflammation caused by two major factors of exposome and appears mediated by AHR-Nrf2. SM activation of CB2R opens a new understanding of SM anti-inflammatory properties.

Keywords: UVA; UVB; pollutants; NQO1; filaggrin; keratin 16; interleukin 6

1. Introduction

As an interface between body and environment, human skin is exposed to interrelated internal and external factors, described by the term “exposome”, which contribute to skin aging process [1]. Intrinsic or chronological aging describes the genetically determined process naturally occurring during life span that can be accelerated by environmental influences, what is called extrinsic aging [2]. Skin is particularly exposed to extrinsic aging, with UV and air pollution being major players of the skin aging exposome [1]. From 2009, Burke and Wei gathered evidence of synergistic damage caused by UVA and pollutants, increasing the risk of skin cancer [3]. Recent works reported the interplay between air pollutants and UV in the disturbance of skin redox homeostasis, inflammation and barrier function alteration [4–6]. Ozone or particulate matter combined to UV demonstrates additive effect in increasing markers of oxidation (lipid peroxidation, heme oxygenase-1 HO-1) and inflammation (transcription factor NF κ B, cyclooxygenase 2 COX2), and in decreasing barrier associated proteins (filaggrin, involucrin). Polycyclic aromatic hydrocarbons (PAHs) or particulate matter and UVA triggers greater phototoxic effect than UV alone, and are associated with reactive oxygen species (ROS) generation and mitochondrial impairments.

ROS are continuously generated in living cells to ensure metabolism and act as intracellular messenger for cell and tissue homeostasis [2]. Maintenance of physiological redox status is controlled by endogenous regulators, notably nuclear factor erythroid 2-related factor 2 (Nrf2) which targets an

array of antioxidant and detoxifying genes as HO-1 and NAD(P)H quinone dehydrogenase 1 (NQO1) [7]. Nrf2 induces those genes by binding a DNA motif called antioxidant response element (ARE).

UV, PAHs, volatile organic compounds, oxides, particulate matter, ozone and cigarette smoke induce oxidative stress in skin and combined pollution exposure has additive effect in the activation of Nrf2 [8,9]. Alteration of oxidative balance is the main driver of skin senescence especially in the epidermis where ROS load is high [10,11]. ROS impair proteins, lipids and DNA by direct oxidation but also induce biological responses: degradation of dermal structural components (collagen, elastin), secretion of inflammatory mediators through NF κ B signaling. This direct relationship between oxidative stress and inflammation which in return generate a pro-oxidative environment, can represent a chronic challenge for the organism exposed to daily environmental insults, called oxinflammation [12].

Aryl hydrocarbon receptor (AHR) is a xenobiotic chemical sensor, expressed in keratinocytes, fibroblasts, melanocytes and T-cell. AHR mediates oxidative response as well as antioxidant pathway in a fine-tuned cross talk with Nrf2 [13]. AHR exogenous ligands include ozone, particulate matter and PAHs [14]. After ligand binding in the cytosol, AHR is translocated to the nucleus, dimerizes with AHR nuclear translocator (ARNT) to bind xenobiotic-responsive element (XRE) of several genes, such as cytochrome P450 1A1 monooxygenase (CYP1A1) which can generate ROS and proinflammatory mediators. On the opposite, natural compounds as flavonoids bind AHR and activate Nrf2-NQO1 pathway which protects cells from ROS-induced oxidative damage. Another role of AHR signaling is the promotion of epidermal barrier function by upregulating genes involved in cornified cell envelop formation such as filaggrin (FLG) through the transcription factor OVO-like 1 (OVOL1) in keratinocytes [15].

Recent findings pointed out the interaction between Nrf2 signaling pathway and cannabinoid receptor type 2 (CB2R) in different biological models and concluded that Nrf2 signaling pathway activation potentiates the effects of CB2R agonists [16–18]. CB2R activation reduces inflammatory cytokines and lesions in psoriasis models through Nrf2 pathway and induces β -endorphin release in keratinocytes so decreasing nociception [19,20].

Topical application of cosmeceutical containing antioxidants appears an efficient strategy to prevent skin barrier damage induced by environmental stressors exposure [5,10,21]. Silymarin (SM) is a seed extract of *Silybum marianum* (L.) Gaertn. (Asteraceae) commonly named milk thistle and renowned for its hepatoprotective properties. SM contains specific flavonoids called flavonolignans, mixing taxifolin and coniferyl alcohol moieties. Dermatological applications of SM are based on its antioxidant properties and protective effects against UV-induced skin damages [22]. Indeed, topical treatment containing SM inhibits photocarcinogenesis in murine model and protects human keratinocytes from UVB induced apoptosis and DNA damages [23]. SM components also has anti-inflammatory properties and decrease the production of LPS-induced pro-inflammatory cytokines in keratinocytes [24]. SM and silibinin, its main constituent (50-70%), exert antioxidant properties at different levels: direct free radical scavenging; inhibition of specific enzymes responsible for free radical production; maintenance of mitochondrial integrity in stress conditions; and activation of antioxidant enzymes and non-enzymatic antioxidants, mainly via transcription factors including NF- κ B and Nrf2 [25,26].

The aim of this study was to explore the antioxidant and anti-inflammatory properties of SM in the context of skin daily exposure to UV and urban air pollution. SM decreased ROS and IL-1 α in RHE exposed to UV and urban dust. A gene expression study suggested activation of Nrf2 and AHR, with antioxidant effector NQO1, and barrier function associated proteins filaggrin and keratin 16. SM induced CB2R and β -endorphin release. A clinical study confirmed SM to improve homogeneity and radiance of skin exposed to UV and air pollution and its positive psychological influence on volunteer's mood through self-evaluation, outperforming cannabidiol.

2. Materials and Methods

2.1. SM composition

SM is a brownish-yellow powder obtained by ethyl-acetate extraction of *Silybum marianum* (L.) Gaertn. seeds. Quantitation of SM extract in silibinin equivalents was achieved by HPLC according to European Pharmacopeia quality control standards. Silibinin A and B, silicristin and silidianin and isosilibinin A and B were quantified. Analysis was performed on Lichrospher RP-18 125x 4mm, 5 µm (Merck) maintained at 25°C. Mobile phases were orthophosphoric acid 85% / methanol / water (0.5/35/65, v/v) and orthophosphoric acid 85% / methanol / water (0.5/50/50, v/v). Flow rate was 0.8 ml/min and injection volume 10 µL. Detection was performed in UV at 288 nm.

2.2. Impact of SM on induced oxidative stress in NHEKs

The cell culture was done on primary cells freshly isolated from biopsies. Normal human skin samples were collected from donor who had given informed consent. Normal Human Epidermal Keratinocytes (NHEKs) were seeded in a black plate with a glass bottom at 20 000 cells per well in 96-wells plates with a type I collagen pre-coating in quadruplicate. The cells were incubated for 24 hours in complete medium (Dermalife medium supplemented with factors) at 37°C with 5% CO₂. Then, the cells were treated in complete medium supplemented with resveratrol (positive control) at 50 µM, or SM at 0.001, 0.005 and 0.01 mg/mL. Skin cells cultivated in complete medium without supplementation were used as negative control. After 24h of incubation at 37°C and 5% CO₂, the 2',7'-Dichlorofluorescein diacetate (DCFH-DA) probe has been added to the wells at 50 µM for at least 30-45 minutes at 37°C. Cells were then washed two times with phosphate buffered saline (PBS) and treated with the oxidative stress inducer, tert-Butyl hydroperoxide solution (TBP), at 5mM in PBS. The untreated cells remained in PBS. Finally, the emitted fluorescence was measured in darkness by excitation wavelength at 488 nm and emission wavelength at 525 nm with microplate reader (TECAN). The study was carried out in quadruplicate (n=4).

2.3. Impact of urban dust and UV exposure on RHE treated with SM

An 8-day-old reconstructed human epidermis (RHE-Lb) of 0.6 cm² was used for this test (Synlevia). Two products were tested: a formulation containing SM 1% (w/w) and the placebo cream (without SM). RHE were treated or not (negative control) with formulations, by topical application, and incubated for 24 hours.

INCI formula: AQUA/WATER, CETYL ALCOHOL, GLYCERYL STEARATE, PEG-75 STEARATE, CETETH-20, STEARETH-20, ISODECYL NEOPENTANOATE, PENTYLENE GLYCOL, PHENOXYETHANOL.

At day 9, the product residue was removed with a swab. RHE were then placed in irradiation medium containing DCFH-DA and incubated for 1 hour. After a medium change to remove DCFH-DA and a topical rinse, RHE were exposed to UVA/B stress (UVA 2.5 J/cm² + UVB 100 mJ/cm²) with or without urban dust (100 µg/ml, topical application, 50 µl/RHE) using BIO-SUN (Vilber). Urban dust corresponds to particulates matter of characterized composition: heavy metals (cadmium, lead, mercury, nickel, vanadium), aluminium, copper, chromium, manganese, chlorinated pesticides, polychlorinated Biphenyl (PCB) congeners, PAHs, nitro-PAHs, dibenzo-p-dioxin and dibenzofuran congeners. Immediately after the stress, RHE were transferred to fresh assay medium (Epilife optimized by Synlevia), and incubated for 6h applying placebo, SM 1% or no treatment, before being processed. Each RHE was cut in two parts. A half RHE was processed for histology and a half RHE was processed for ROS quantification. RHE media (subnatants) were collected and stored at -20°C before IL-1a quantification by ELISA or treatment of NHEKs for gene expression analysis. All experimental conditions were performed in triplicate (n=3).

Histological analysis was conducted on fixed tissues, dehydrated in multiple baths with increasing concentrations of ethanol, and then embedded in paraffin. Transversal sections were performed with a microtome (5 µm thickness, 1 slide per labeling) and maintained at room

temperature. The sections were then deparaffinized and stained according to the standard protocol of HE (hematoxylin eosin) staining. Briefly, sections were stained with hematoxylin, rinsed and stained with eosin. The sections were then rinsed and mounted in aqueous medium.

To achieve ROS quantification, RHE were embedded in OCT (optimal cutting temperature) medium and frozen at -80°C until blocks were processed for sectioning in a cryostat and mounted on slides. Tissue sections were observed using a ZEISS 710 confocal microscope. Images were captured and processed with ZEN software (objective lens x20). The fluorescence intensity was quantified using ImageJ software and normalized to the living layer area of the epidermis (i.e., excluding the stratum corneum) identified by DAPI staining of nuclei. Three image per replicate were captured.

Quantification of IL-1a in RHE subnatants was performed according to the kit manufacturer's instructions (R&D Systems # DY200-05, standard curve range: 7.8-500 pg/ml).

2.4. Gene expression study on NHEKs treated with stressed RHE conditioned medium

Keratinocytes were seeded in a 24-well plate and cultured for 24 hours in culture medium and was then replaced by assay medium containing, or not (control), the conditioned media of RHE for further 24 hours of incubation. Conditioned media were tested at 50%. The following experimental conditions were tested: stressed conditioned medium from non-treated RHE stressed with UV and urban dust and stressed conditioned medium from RHE stressed with UV and urban dust and treated with SM 1%. At the end of incubation, the cells were washed in PBS solution and immediately frozen at -80°C. All experimental conditions were performed in triplicate (n=3).

Gene expression analysis was realized by RT-qPCR method on total RNA extracted from the cell monolayers of each experimental condition. Total RNA was extracted from each sample using TriPure Isolation Reagent® according to the supplier's instructions. The quality of RNA was evaluated using capillary electrophoresis (Bioanalyzer 2100, Agilent technologies). The quantity of RNA was evaluated using a spectrophotometer (Synergy H1, BioTek Instruments). The complementary DNA (cDNA) was synthesized by reverse transcription of total RNA in presence of oligo(dT) and « Transcriptor Reverse Transcriptase » (Roche). The cDNA quantities were then adjusted before qPCR step. The qPCR was performed using a LightCycler® system (Roche Molecular Systems Inc.) according to the supplier's instructions. Reaction mix (10 µL) was prepared as follows: 2.5 µL of cDNA, primers (forward, reverse) and reagent mix (Ozyme) containing Taq DNA polymerase, SYBR Green I and MgCl₂. Reference gene Actin Beta (ACTB) was used for data normalization.

2.5. Activation of human CB2R by CBD or SM: EC50 determination

The activation of the CB2R has been evaluated on human recombinant CB2R. Several concentrations of CBD or SM or 100 nM of WIN 55212-2, a CB2R agonist, or no treatment (control) have been applied during 10 minutes at 37°C and cAMP was measured by HTRF to evaluate the EC50. The EC50 values (concentration producing a half-maximal response) were determined by non-linear regression analysis of the concentration-response curves generated with mean replicate values using Hill equation curve fitting where Y = response, A = left asymptote of the curve, D = right asymptote of the curve, C = compound concentration, and C₅₀= EC50 and nH = slope factor.

$$Y = D + \frac{A - D}{1 + \left(\frac{C}{C_{50}}\right)^{nH}}$$

This analysis was performed using software developed at Cerep (Hill software) and validated by comparison with data generated by the commercial software SigmaPlot® 4.0 for Windows® (© 1997 by SPSS Inc.). Cellular agonist effect was calculated as a percentage of control agonist response (WIN 55121-2) for each target, and cellular antagonist effect was calculated as a percentage of inhibition of control reference agonist response for each target.

2.6. Activation of human CB2R by CBD or SM in mast cells and β -endorphin release

Human Mast Cells (HMC1.1) have been isolated from fresh skin biopsies (SCC097, Sigma) and treated for 16 hours with CBD at 0.0025mg/mL or SM at 0.05mg/mL (w/v). Cells were then incubated at 37°C, 5% CO₂. After 16 hours, supernatant was collected for further ELISA analysis and cells were trypsinised and counted with Luna cell counter. Release of cAMP and β -endorphin by mast cells was quantified using ELISA kits and following supplier recommendation (Abcam).

2.7. Clinical study: impact of SM on urban skins and comparison with cannabidiol

Double blind, placebo controlled clinical study has been carried on 68 women aged between 45 and 75 years old. All the subjects participating gave their informed consent signed at the beginning of the study. The study followed and was in compliance with the tenets of the Declaration of Helsinki. The volunteers are living in a dense urban environment in Thailand and are thus exposed both to UV rays and pollution (Spincontrol Asia). The volunteers applied twice a day for 56 days a placebo formula or formula with SM 1% or formula with CBD 0.02%.

The INCI formula composition was as follows: AQUA, CETHYL ALCOHOL, GLYCERYL STEARATE, PEG-75 STEARATE, CETETH-20, STEARETH-20, PENTYLENE GLYCOL, ISODECYL NEOPENTANOATE, +/- SILYBUM MARIANUM FRUIT EXTRACT, CAPRYLIC / CAPRIC TRIGLYCERIDE, CITRIC ACID, DIMETHICONE, SODIUM BENZOATE, AMMONIUM ACRYLOYLDIMETHYLTAURATE/BEHENETH-25 METHACRYLATE CROSSPOLYMER, FRAGRANCE, +/- CANNABIDIOL 99%

Inclusion criteria for the recruitment of panelists were: female subjects, 45-75 years of age, exposed to UV rays and pollution several times a day, all skin type at least 1 subject by skin type, having sensitive skin based in stinging test, having underneath eye wrinkles with a grade ≥ 4 according to the Skin Atlas (pp. 47) and having dull complexion according to the C.L.B.T. scale from Spincontrol Asia.

Digital photography using VISIA CR2.3® were taken to analyze skin homogeneity and radiance and the volunteer have completed a well-being questionnaire analyzed by Emospin. The Well-being Questionnaire (W-BQ) has been originally constructed to measure psychological well-being in people with a chronic somatic illness. Because of its versatility and robustness, this tool is recommended by the World Health Organization for widespread use [27].

2.8. Statistical analysis

For *in vitro* and *ex vivo* studies, a Shapiro-Wilk normality test has been performed to evaluate whether the data follow the Gaussian Law. If the results have a normal distribution, Student's t-test statistical analysis was performed. If the results did not follow the Gaussian Law, a non-parametric statistical analysis was performed by Kruskal-Wallis ANOVA followed by Mann Whitney U test.

All raw data from *in vivo* experiments were analyzed by Shapiro-Wilk test in order to determine if the data followed Gaussian law or not. If yes, data were analysed using parametric paired or unpaired Student's t-test. If not, data were analysed using non-parametric Wilcoxon test or non-parametric Mann-Whitney test. Self-assessment has been analysed by contingency method using Chi square test with ** $p < 0.01$.

A result is considered as significant if $p < 0.1$, $p < 0.05$ *, $p < 0.01$ ** and $p < 0.001$ ***.

3. Results

3.1. SM composition

SM is a standardized extract of *Silybum marianum* (L.) Gaertn. seeds, enriched in flavonolignans. In this study, the main phenolic compounds were identified as silibinin A and B, constituting 56% of SM. As previously reported [22], the studied SM also contained minor flavonolignans: silicristin and silidianin representing 30.3% of the extract and isosilibinin A and B, 13.8%.

3.2. SM reduced ROS during oxidative stress on NHEKs

ROS are generated as a first response to environmental stressors in skin [28]. SM has oxidant scavenging properties and decrease UV-induced oxidative stress [22,23]. Here this activity was observed on NHEKs model treated with oxidative stress inducer, TBP, at 5 mM. In TBP treated NHEKs, the amount of ROS significantly increased by 82% (Figure 1). Pre-treatment with a positive antioxidant control, resveratrol, lead to reduce ROS by 63% compared to TBP treated cells. SM at 0.001 mg/mL did not modify ROS quantity. SM at 0.005 mg/mL and 0.01 mg/mL significantly reduced ROS in a dose dependent manner, -16% and -34% respectively compared to TBP treated condition. Preliminary studies demonstrated that SM 0.01 mg/mL did not impact cell viability on MTT assay (3-(4,5-dimethylthiazol-2-yl)-2,5-diphenyltetrazolium bromide) with 90% of viability vs non treated condition. These data confirm SM has antioxidant properties in epidermal cells.

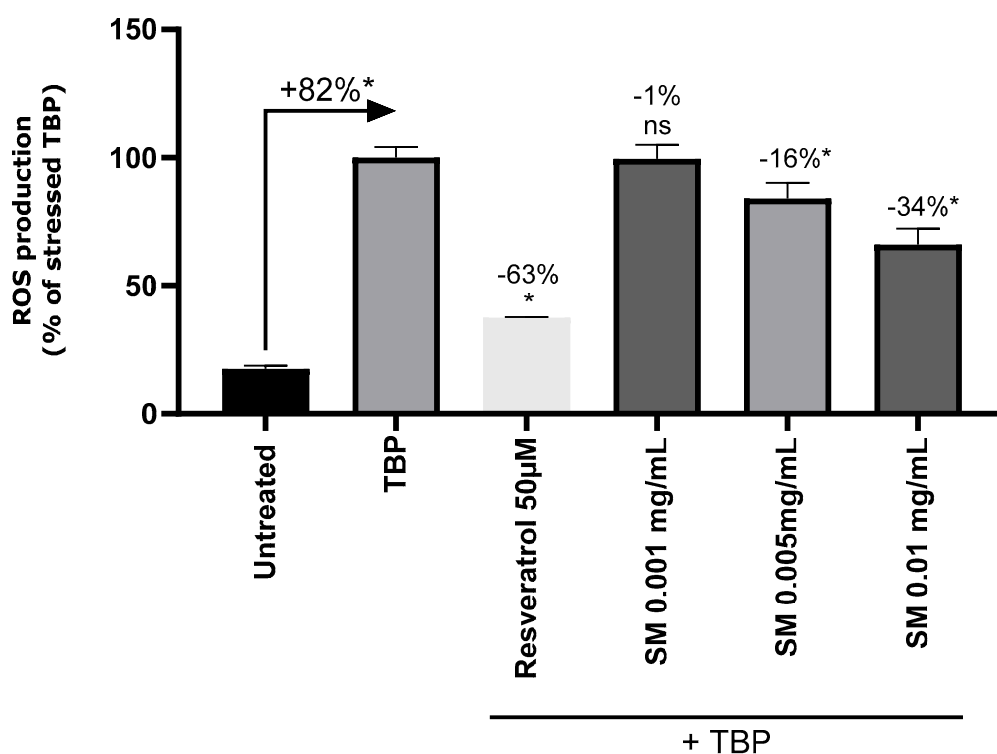


Figure 1. Quantification of Reactive Oxygen species (ROS) in Normal Human Epidermal Keratinocytes (NHEKs) without treatment (untreated), treated with tert-Butyl hydroperoxide (TBP) 5 mM, and pretreated with resveratrol 50 µM (positive control) or Silymarin (SM) at 0.001 mg/mL, 0.005 mg/mL or 0.01 mg/mL before TBP application. Results are expressed in percentage of condition stressed with TBP. Mann-Whitney test, $p < 0.1$ #, $p < 0.05$ *, $p < 0.01$ ** and $p < 0.001$ ***.

3.3. SM maintain normal phenotype on [UVA/B+Urban Dust] stressed RHE

The additive effect of UV and air pollutants was previously demonstrated [4,5]. RHE were treated with SM 1% in formulation or placebo before and after exposure to UVA/B and urban dust. Morphological changes analysis and ROS and IL-1 α quantification allowed the comparison of untreated, placebo and SM conditions.

Morphological analysis is presented in Figure 2. Control RHE (untreated) exhibited a normal phenotype characterized by a multi-layered epidermis showing tissue differentiation from the basal layer to the *stratum corneum* with the presence of many grains of keratohyalin in the granular layer. Tissues stressed with UVA/B and urban dust were disorganized and exhibited a pathological morphology presenting pycnotic nuclei and spongiosis (intercellular edema), especially in the basal layer. Topical application of SM decreased pycnotic nuclei and spongiosis while the placebo had no impact on the phenotype induced by UVA/B and urban dust exposure.

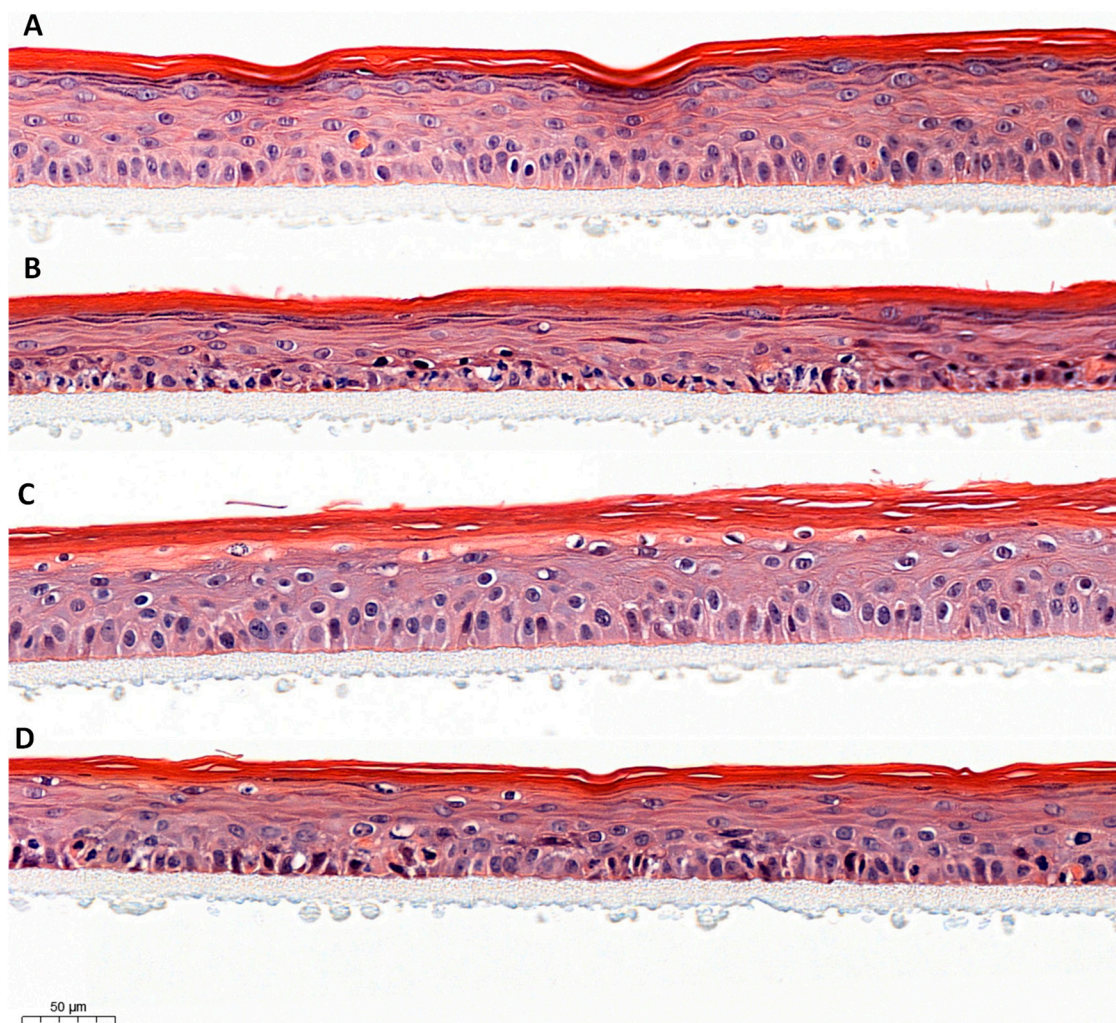


Figure 2. Comparison of Reconstructed Human Epidermis (RHE) morphology: untreated control (A), exposed to UVA/B and urban dust (B), treated with Silymarin 1% (C) or placebo (D) by topical application before and after exposition to UVA/B and urban dust.

3.3. SM reduced ROS on [UVA/B+Urban Dust] stressed RHE

ROS were quantified in RHE in order to evaluate the oxidative stress induced by UVA/B and urban dust application and confirmed the antioxidant properties of SM. Representative pictures of ROS analysis by fluorescence confocal microscopy are presented in Figure 3 and quantitative data are charted in Figure 4. Exposition of RHE to UVA/B and urban dust increased ROS content by +539% compared to untreated condition. Placebo treated RHE exhibited similar increase in ROS content. Applying SM at 1% in cream significantly reduced ROS production by -295% vs untreated stressed condition. The results confirm the ability of SM to reduce the ROS production in epidermis under combined exposure to common daily environmental stress.

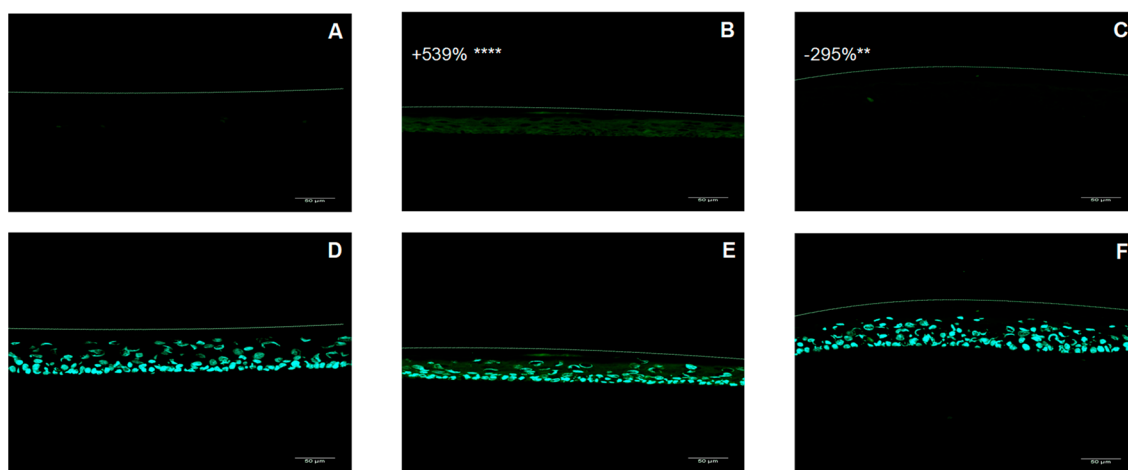


Figure 3. Representative pictures of fluorescence confocal microscopy for reactive oxygen species detection by dichlorofluorescein (DCF) (A, B, C) and 4',6-diamidino-2-phenylindole (DAPI) staining (D, E, F) in untreated Reconstructed Human Epidermis (RHE) (A, D), stressed with UVA/B and urban dust (B, E), and treated with formulation containing Silymarin 1% (C, F). Percentage is expressed in comparison to unstressed control except for Silymarin treated condition for which decrease is expressed in comparison to UVA/B and urban dust stressed condition. Mann Whitney U test, $p < 0.1\#$, $p < 0.05^*$, $p < 0.01^{**}$ and $p < 0.001^{***}$.

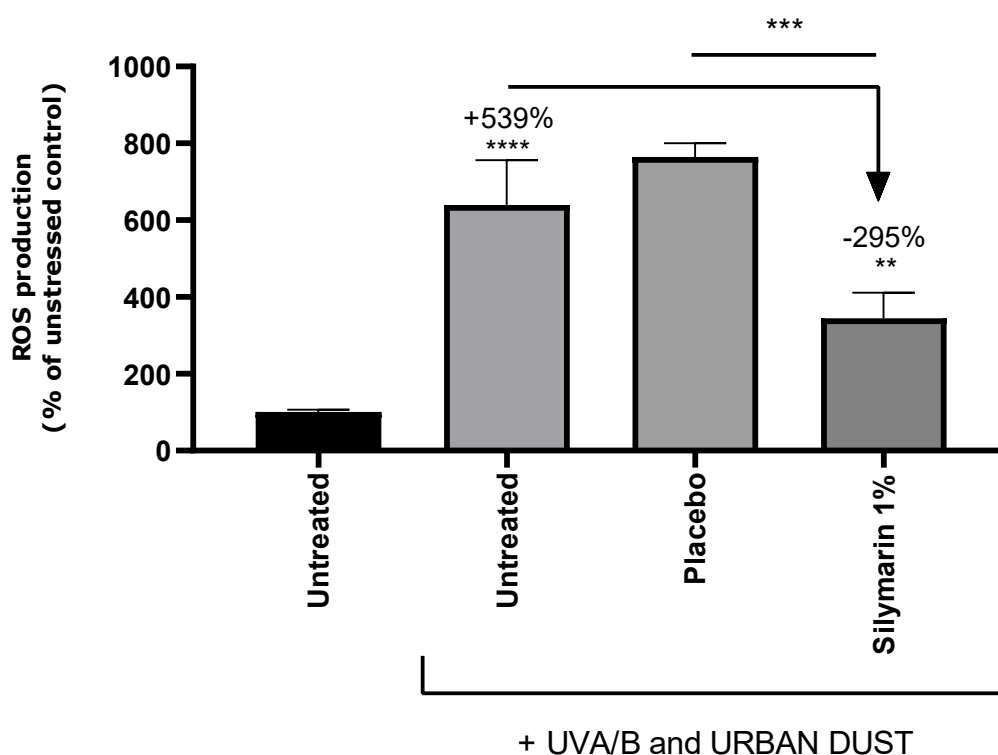


Figure 4. Quantification of reactive oxygen species in untreated Reconstructed Human Epidermis, stressed with UVA/B and urban dust, and treated with placebo cream or formulation containing Silymarin 1%. Percentage is expressed in comparison to unstressed control except for Silymarin treated condition, for which decrease is expressed in comparison to UVA/B and urban dust stressed condition. Mann Whitney U test, $p < 0.1\#$, $p < 0.05^*$, $p < 0.01^{**}$ and $p < 0.001^{***}$.

3.4. SM reduced IL-1 α on [UVA/B+Urban Dust] stressed RHE

IL-1 α is a pro-inflammatory cytokine highly expressed in the skin and produced by keratinocytes. It is considered as a key player initiating the development of inflammatory response [29]. Stress induced by UVA/B and urban dust increased by 213% the quantity of IL-1 α in the subnatants of RHE (Figure 5). Similar values were obtained on the subnatants of RHE treated with placebo formulation. SM 1% cream decreased by -81% IL-1 α amount compared to the untreated stressed RHE. These data confirm SM has anti-inflammatory properties in this context.

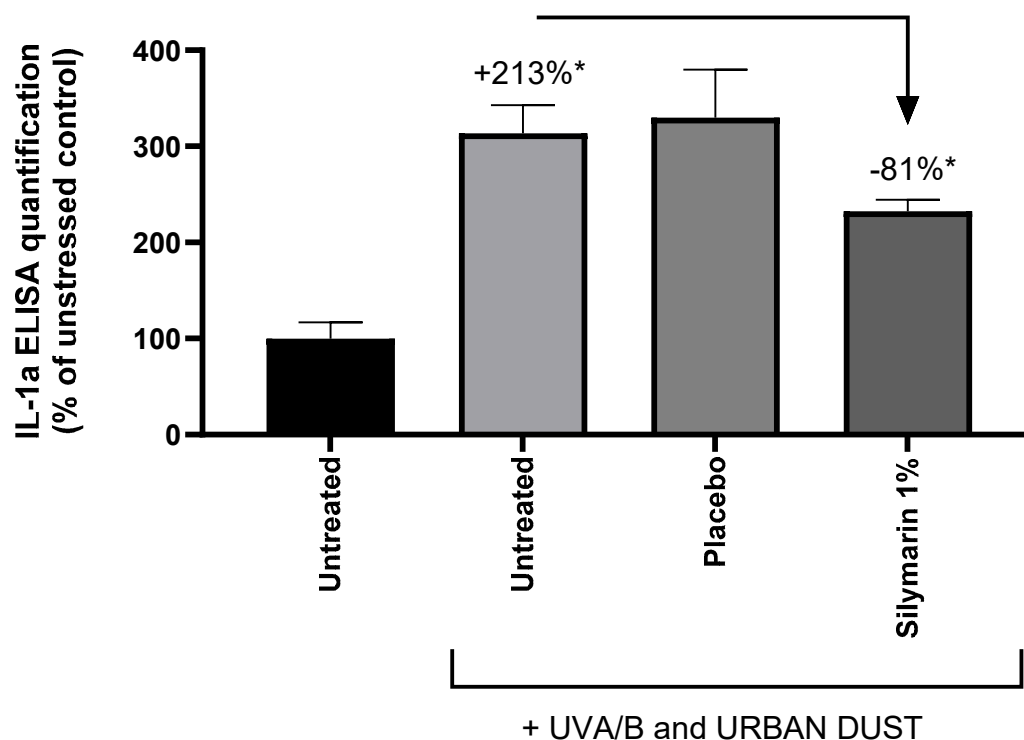


Figure 5. Quantification of interleukin 1 alpha (IL-1 α) by enzyme-linked immunosorbent assay (ELISA) in untreated Reconstructed Human Epidermis, stressed with UVA/B and urban dust, and treated with placebo cream or formulation containing Silymarin 1%. Percentage is expressed in comparison to unstressed control except for Silymarin treated condition for which decrease is expressed in comparison to UVA/B and urban dust stressed condition. Mann Whitney U test, $p < 0.1$ #, $p < 0.05$ *, $p < 0.01$ ** and $p < 0.001$ ***.

3.5. SM upregulated AHR and Nrf2 pathways

In order to understand the mode of action of SM that underlies its antioxidant and anti-inflammatory properties, the conditioned medium of stressed RHE treated with SM, was used to stimulate NHEKs. A gene expression study was conducted to determine the genes that were upregulated or downregulated compared to stimulation by the conditioned medium from untreated stressed RHE (Figure 6).

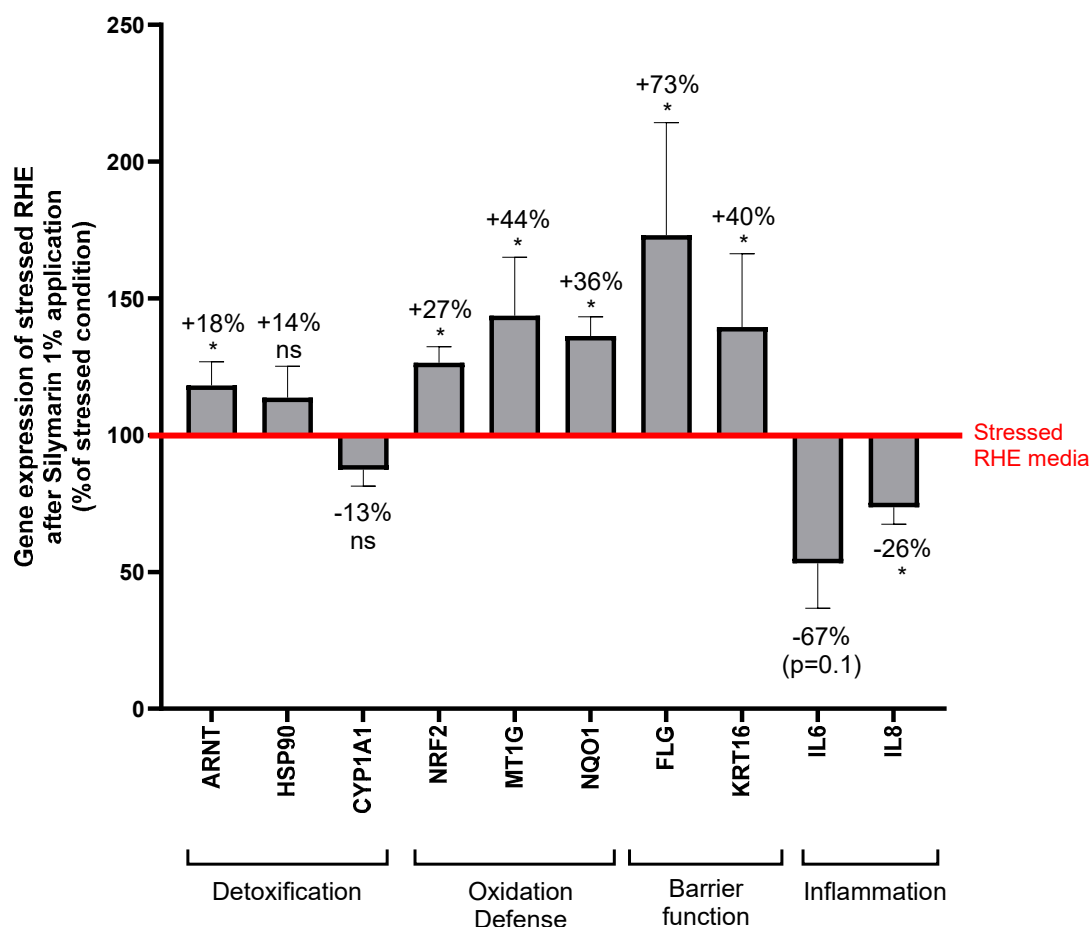


Figure 6. Relative gene expression of Normal Human Keratinocytes treated with conditioned medium of stressed Reconstructed Human Epidermis (RHE) treated with Silymarin 1% before and after exposure to UVA/UVB and urban dust. Values are relative to the conditioned medium of stressed RHE without treatment. *ARNT*: AhR nuclear translocator, *HSP90*: heat shock protein 90, *CYP1A1*: cytochrome P450 1A1 monooxygenase, *NRF2*: nuclear factor erythroid 2-related factor 2, *MT1G*: metallothionein 1G, *NQO1*: NAD(P)H quinone dehydrogenase 1, *FLG*: filaggrin, *KRT16*: keratin 16, *IL-8*: interleukin 8, *IL-6*: interleukin 6. Mann Whitney U test, $p < 0.1$, $p < 0.05$ *, $p < 0.01$ ** and $p < 0.001$ ***.

Interleukin 8 gene (*IL-8*), encoding a chemokine produced during oxidative stress induced by UV rays and pollutants, was significantly downregulated. Interleukin 6 gene (*IL-6*), encoding a pro-inflammatory cytokine, was close to be significantly downregulated. Expression of *CYP1A1*, coding for a monooxygenase involved in the detoxication of carcinogens through AhR pathway, was not modified by SM treatment.

Six genes were significantly upregulated and encodes the following proteins: ARNT complexing AhR in the nucleus; nuclear factor Nrf2 regulating oxidative stress and inflammation; NQO1, a target gene of Nrf2, regulating cellular redox state through quinone detoxification; Metallothionein 1G (MT1G) involved in the response to metallic ion; filaggrin (FLG) a structural protein involved in epidermal barrier function; and finally keratin 16 (KRT16) a type I keratin associated to wound repair, proliferation and inflammation.

These results indicates that SM potentially activated AHR pathway without inducing its target *CYP1A1*. The increased expression of *FLG* and *KRT16* indicates a regulation of the epidermal barrier function by the plant extract. This is consistent with AHR and Nrf2 activation: AHR regulates *FLG* through the transcription factor OVO-like 1 (OVOL1) in keratinocytes and Nrf2 controls *KRT16* [15,30]. Up-regulation of *FLG* and *KRT16* is also in accordance with the maintenance of a normal epidermal morphology in SM treated RHE. Nrf2 pathway was also probably activated as demonstrated by *Nrf2*

and *NQO1* upregulation. *MT1G* promoter contains the anti-oxidant response element [31], suggesting it could be regulated by Nrf2, and reinforce our hypothesis. The decrease of *IL-8* and *IL-6* expression was expected as they are regulated by IL-1 α [32,33] and it tends to confirm the anti-inflammatory activity of SM.

3.5. SM activated human CB2R

A recombinant human CB2R was used to test the ability of SM to reduce the release of cAMP and so activate CB2R, *in vitro*. A comparison with CBD was made. The EC₅₀ of the reference agonist WIN55212-2 was 9.93 10⁻⁵ μ g/mL. The EC₅₀ of SM was determined at 76.0 μ g/mL and that of CBD at 55.4 μ g/mL demonstrating a moderate agonist effect of both compounds on CB2R.

3.5. SM activated CB2R in mast cells and induced β -endorphin release

Mast cells are immune cells having an important role in the first-line defense of skin and in the regulation of barrier function [34,35]. They express cannabinoid receptor type 2 (CB2R) as keratinocytes and appeared as a good model to test the potential SM agonist effect [36]. Both SM and CBD activated the receptor (Figure 7).

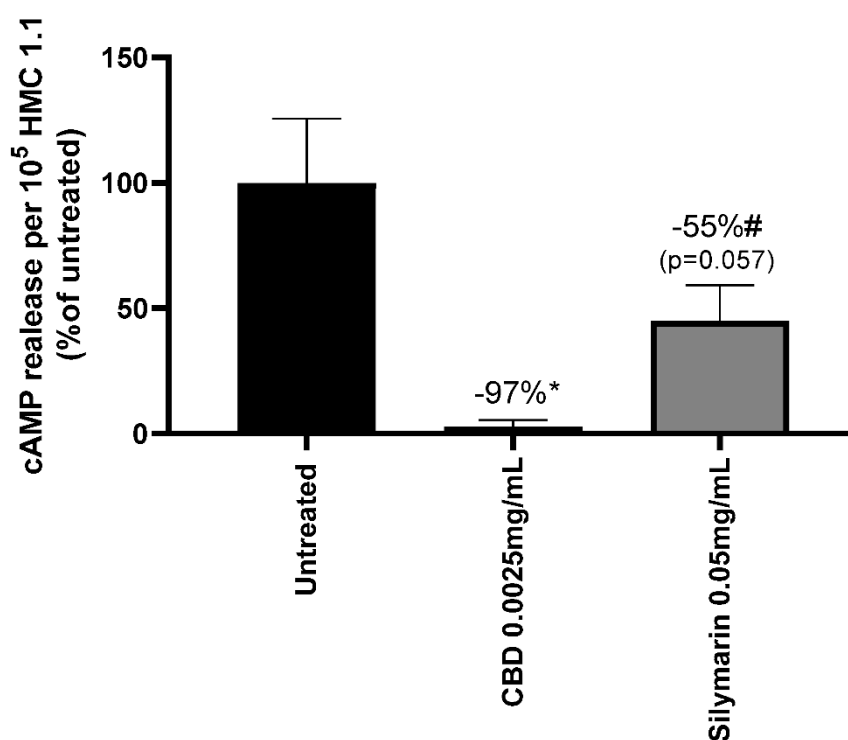


Figure 7. Activation of cannabinoid receptor type 2 (CB2R) in mast cells (HMC1.1) measured through the inhibition of cAMP release by cannabidiol (CBD) and Silymarin. Results are expressed in percentage of the untreated cells. Mann-Whitney test, p<0.1#, p<0.05*, p<0.01** and p<0.001***.

Ibrahim et al. demonstrated that CB2R activation in keratinocytes lead to the release of β -endorphin [20]. The endogenous opioid was quantified in mast cells treated with CBD or SM in presence or absence of a CB2R antagonist, SR144528, to confirm that β -endorphin release depends on CB2R activity. Both CBD and SM increased β -endorphin release from mast cells by +17% and +19% respectively compared to untreated cells. The use of SR144528 CB2R antagonist did not modify β -endorphin release from CBD treated mast cells while it decreased by -23% in SM treated mast cells. This confirms that Silymarin activity on β -endorphin secretion is correlated to CB2R activation which is not verified for CBD.

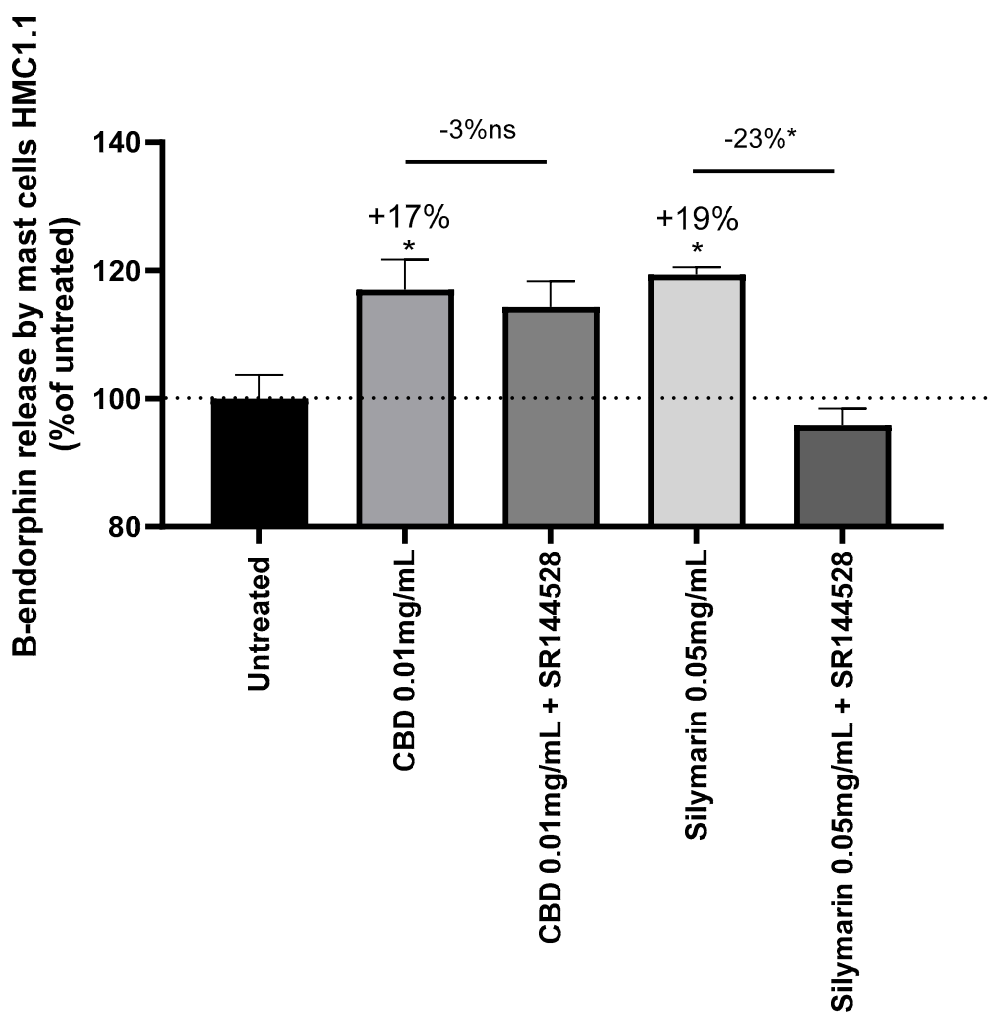


Figure 8. Quantification of β -endorphin (B-endorphin) release by mast cells (HMC1.1) induced by cannabidiol (CBD) and Silymarin. SR144528 is a CB2R antagonist. Results are expressed in percentage of untreated cells response. Decrease of β -endorphin release in CBD/SR144528 and Silymarin/SR144528 treated cell is expressed relatively to CBD and Silymarin treated cells. Mann-Whitney test, $p < 0.1$ #, $p < 0.05$ *, $p < 0.01$ ** and $p < 0.001$ ***.

3.5. SM improved homogeneity and radiance of skins exposed to UV and air pollution

Double blind vs placebo clinical study was conducted on 68 women, 45 to 75 years old, daily exposed to UV rays and air pollution, presenting sensitive skin and dull complexion according to C.L.B.T. (coloring, luminosity, brightness and transparency) scale. Placebo cream or formulation containing 0.02% CBD or 1% SM, were applied twice a day for 56 days. Skin homogeneity and radiance were evaluated at the last day of application. A well-being questionnaire allowed to measure the impact of actives on panelists energy perception.

CBD activates antioxidant pathways regulating inflammation in keratinocytes and mediates epidermal differentiation through AHR signaling [37,38] and is considered as potential therapeutic for inflammatory skin disorders [39]. CBD is today commercialized as cosmetic active fighting inflammation and oxidative stress in sensitive skins. That is why CBD was selected as a benchmark for this study.

Skin homogeneity, defined as facial skin color distribution and skin smoothness in texture, was measured at day 56 and compared to day 0 (Figure 9). SM 1% induced an increase in skin homogeneity vs day 0, by 1.6 factor compared to placebo, and by 2.7 factor compared to CBD. On top of that, skin homogeneity improvement was effective in 91% of panelist using SM formula, 52% of panelists using CBD cream and 72% of panelists applying placebo. These results are illustrated by

representative pictures of panelist applying SM containing cream (Figure 10 A): the blue spots indicating heterogeneous areas are attenuated along the study course showing improvement in skin smoothness and color homogeneity; while changes were not conspicuous for panelists applying CBD or placebo formulations (Figure 10 B and 10 C respectively). The measurement of skin radiance (Figure 9) supported findings on skin homogeneity: only SM 1% in cream helped to significantly improve skin luminosity (x1.6 vs CBD).

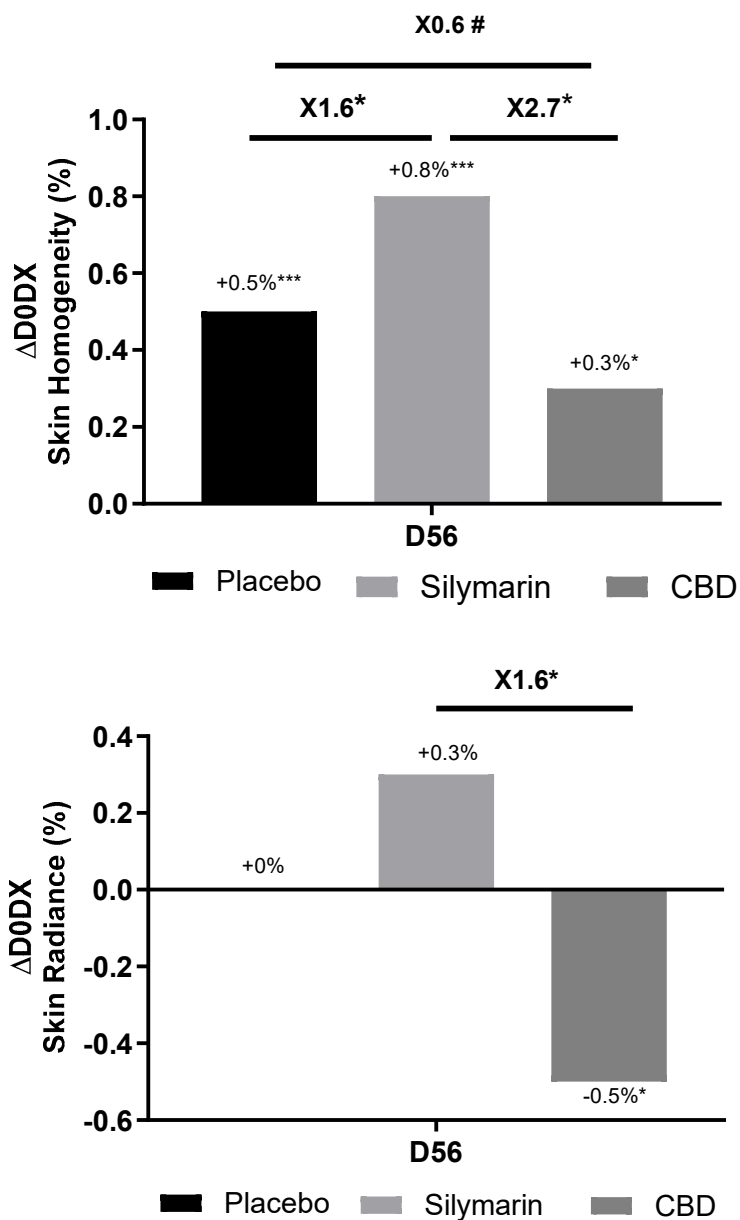
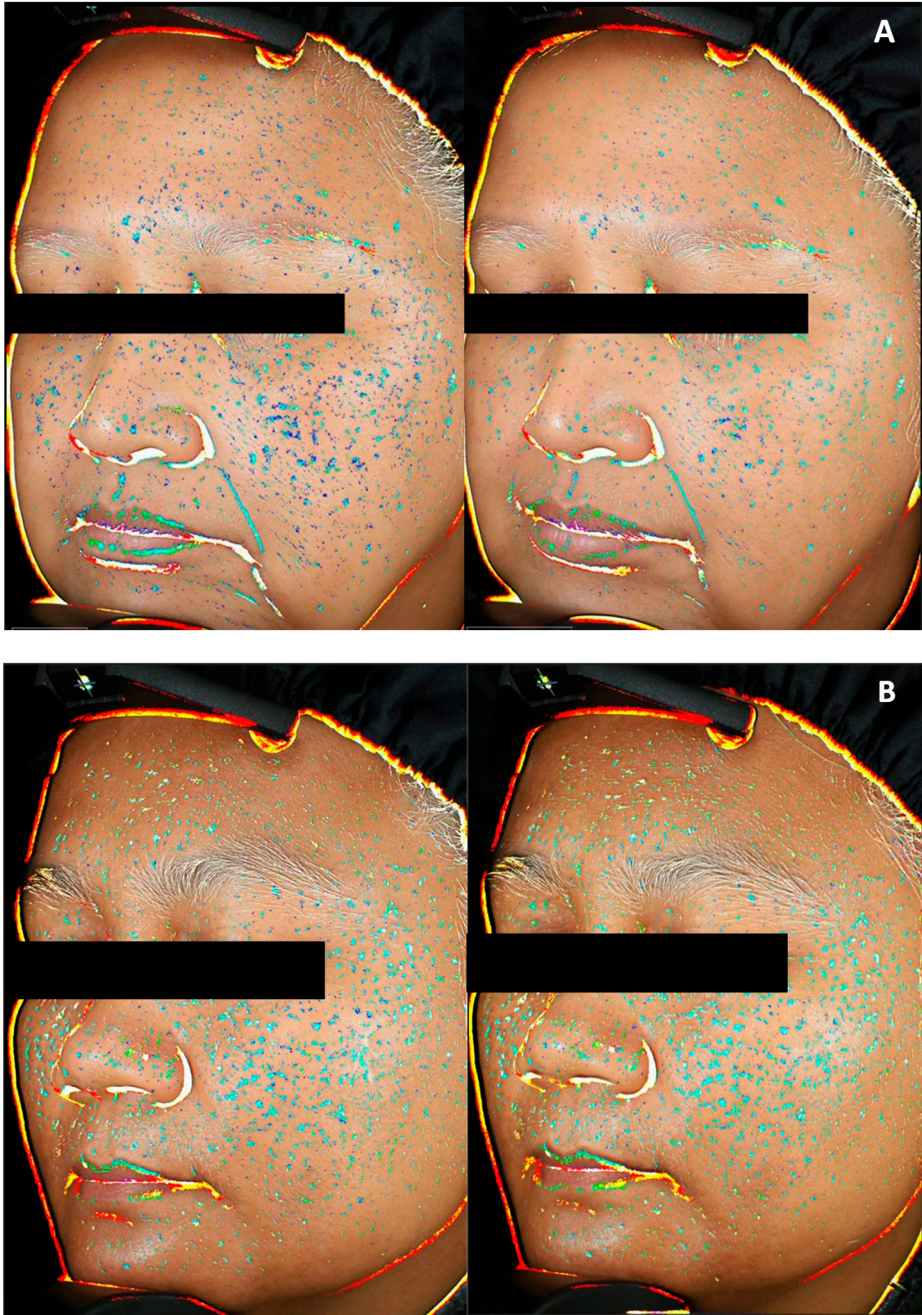


Figure 9. Comparison of skin homogeneity (up) and radiance (down) at 56 (D56) vs day 0 (D0) between groups applying placebo cream or Silymarin 1% in formulation or cannabidiol (CBD) 0.02% in formulation. Wilcoxon test vs D0, Mann Whitney test vs placebo, $p < 0.1$ #, $p < 0.05$ *, $p < 0.01$ ** and $p < 0.001$ ***.



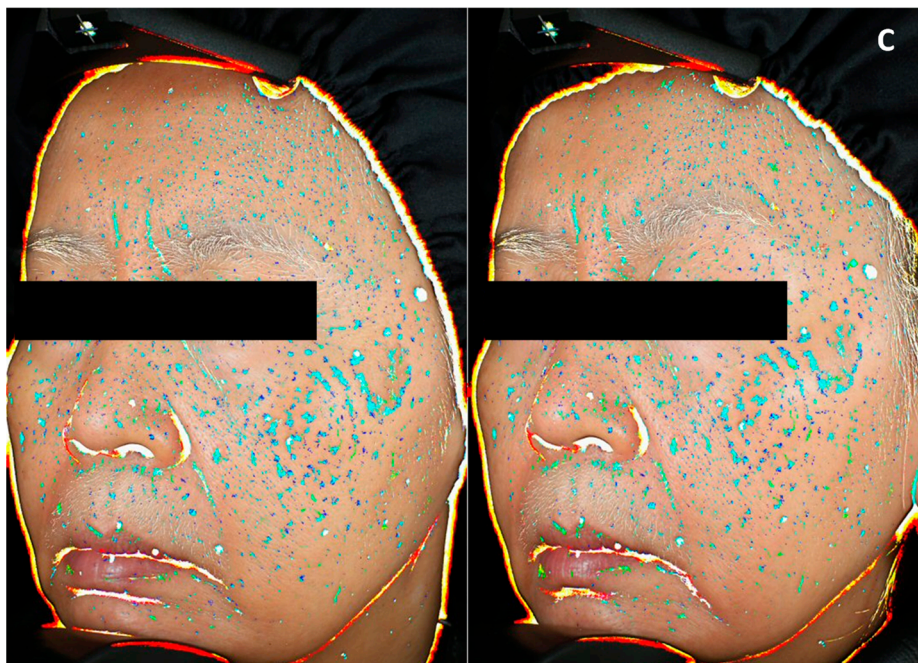


Figure 10. Representative pictures illustrating skin homogeneity changes at day 0 (left) and day 56 (right), of panelist applying Silymarin 1% in formulation (A) or cannabidiol 0.02% in formulation (B) or placebo cream (C). Heterogeneity is indicated by blue spots: light blue representing the highest contrast to dark blue representing the lowest contrast.

Volunteers completed a well-being questionnaire analyzed by Emospin. SM significantly improved energy well-being, in other word, positive mood dynamic, in a similar manner as cannabidiol compared to placebo (Figure 11).

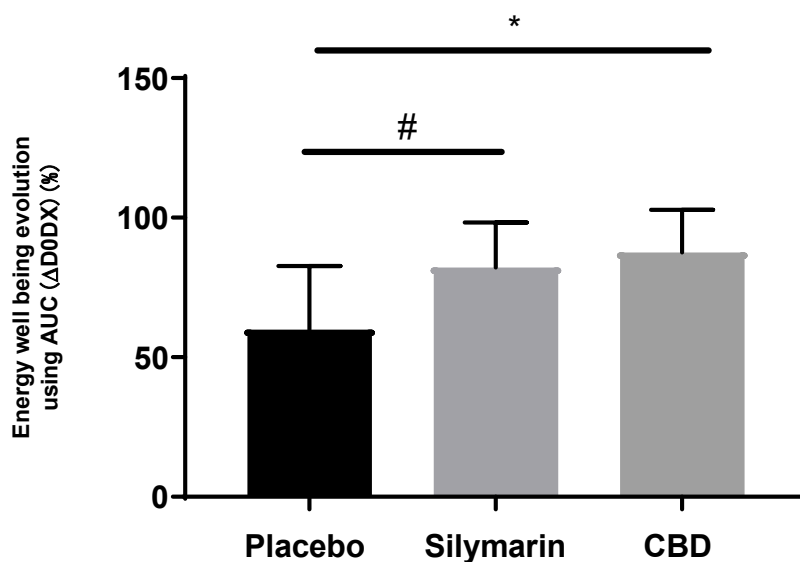


Figure 11. Quantitative data extracted from well-being questionnaire and comparing the evolution of volunteers' self-evaluation of their skin energy. Mann Whitney test vs placebo, $p < 0.1\#$, $p < 0.05^*$, $p < 0.01^{**}$ and $p < 0.001^{***}$.

4. Discussion

Skin is particularly exposed to ultraviolet radiation (UV) and air pollution which are major players of the skin aging exposome [1]. Recent works demonstrated the interplay between air pollutants and UV in the disturbance of skin redox homeostasis, inflammation and barrier function alteration resulting in oxinflammation [4–6].

In our study, RHE stressed by a combination of UV and urban dust presented morphological alterations, increased ROS and IL-1 α contents suggesting oxidative stress and inflammation. IL-1 α is constitutively secreted as precursor protein in keratinocytes, and rapidly increases under UVB exposure, inducing the release of IL-6, IL-8 and inflammatory responses [32,33]. In double-stressed RHE, SM maintained a normal tissue organization, decreased ROS and IL-1 α , as well as the expression of IL-6 and IL-8. Frankova et al. suggested that anti-inflammatory properties of SM are at least supported by silibinin, a major flavonolignan of SM, which tend to decrease IL-1 α , IL-8 and IL-6 during SDS induced inflammation in RHE.

Nrf2 is a master regulator of cellular antioxidant defenses and its activation appears an interesting strategy to prevent skin from damaged caused by combined exposure to pollution and sun [40]. Indeed, Nrf2 mediates induction of a set of detoxifying and antioxidant enzymes such as NQO1 by binding a DNA sequence called antioxidant response element (ARE) [7]. Moreover, oxidative stress is mediated by a fine-tuned cross talk between AHR and Nrf2 modulated by antioxidant phytochemicals divided in three groups: Nrf2 agonist with AHR agonistic activity, Nrf2 agonist with AHR antagonistic activity, Nrf2 agonist with CYP1A1 inhibitor activity [13]. According to our results, the antioxidant activity of SM was associated with an upregulation of Nrf2 and NQO1 together with genes involved in AHR activation (ARNT), suggesting agonistic activity on both pathways, and did not modify CYP1A1 expression. SM seems to belong to the group of Nrf2 agonist with AHR agonistic activity gathering soybean tar, *Opuntia ficus-indica* extract, *Houttuynia cordata* extract, *Bidens Pilosa* extract, all containing high flavonoid content as SM. Flavonoids are present in several dietary sources and about 6000 structures have been identified. These phenolic compounds are clearly identified as Nrf2 activators [41] and today attract attention for the prevention and treatment of neurodegenerative disorders, cancer or COVID-19 [42–44]. Structure activity relationship study among flavonoids for Nrf2 induction would be of particular interest to determine the effect of the peculiar structure of SM flavonolignans combining taxifolin and coniferyl alcohol.

Under environmental stress, SM increased expression of genes encoding barrier function associated proteins, filaggrin and keratin 16. UV exposure decreases filaggrin content in the epidermis and this effect is aggravated and prolonged by combination to particulate matter exposure [5]. Filaggrin is genetically mapped to the epidermal differentiation complex (EDC) locus, comprising genes encoding proteins involved in the terminal differentiation and cornification of keratinocytes [45]. EDC genes expression, including filaggrin, is modulated by UV and pollutants themselves activating AHR and accelerating keratinocytes differentiation via OVO-like 1 transcription factor [15]. Keratin 16 is transiently expressed in keratinocytes under Nrf2 activation, in the event of a barrier breach and regulates epithelial inflammation and keratinocyte proliferation serving wound repair [30,46]. Collectively these data support the hypothesis of AHR and Nrf2 activation by SM. Several studies report the direct crosstalk between AHR and Nrf2: AHR binding the xenobiotic-responsive element (XRE) of Nrf2, or the last interacting with cap'n'collar-small MAF binding element of AHR promoter. An indirect way involves AHR induced expression of cytochrome P450, releasing intermediate metabolites and then oxidative stress triggering Nrf2 [47].

Recent findings established evidence for CB2R and Nrf2 interaction. CB2R promoter region contains ARE element and is effectively regulated by Nrf2 in microglial cells [16]. Agonists of CB2R induce Nrf2 in skeletal muscle [17] and murine obesity model with anti-inflammatory effect [48]. In diabetic mice, Nrf2 activation potentiates the effect of CB2R agonist [18].

In skin, CB2R is mainly localized in cutaneous nerve fiber bundles, mast cells and in a lesser extent in epidermal keratinocytes [36]. CB2R activation stimulates release from keratinocytes of β -endorphin, which acts at local neuronal μ -opioid receptors to inhibit nociception [20]. CB2R deficiency exacerbates psoriasis symptoms and its agonists improves lesions, decreases inflammatory

cytokines and oxidative stress through Nrf2 [19,49]. Anti-inflammatory properties of CB2R were also confirmed in skin wound healing process [50]. CBD is a major compound of *Cannabis sativa* L. which does not show psychoactivity but has potential to treat skin disorders due to its antioxidative and anti-inflammatory properties previously reviewed [39,51]. CBD reduces oxidative stress in normal human keratinocytes and induces CB2R that is also promoted by UVA and UVB [52]. Moreover, UV stressed 2D and 3D skin models exhibited cytoprotective response when treated with CBD [53].

We hypothesized that part of the anti-inflammatory activity of SM could be related to CB2R induction. In a first assay, SM was shown to be a weak agonist of human CB2R, similarly to CBD. Further tests were conducted on mast cells which appeared as an appropriate model as it plays a key role in immunity and microbiota management thanks to AHR [34], in maintenance of epidermal barrier function [35], and some evidence suggests the role of CB2R in immune modulatory effects during inflammation [50,54]. Very interestingly, SM was found to activate CB2R and induced release of β -endorphin from mast cell in a similar way as CBD. This opens a new area of research on the understanding of anti-inflammatory and antioxidant properties of SM.

Solar radiation and air pollution cause premature ageing through several clinical signs: pigmentary changes including lentigines, wrinkles, roughness, skin pores, skin redness, rosacea; altering skin homogeneity [28]. A radiant complexion means healthy and young skin and influences facial attractiveness [55,56]. SM significantly improved skin homogeneity on 91% of volunteers who felt positive impact on their energy well-being, reflecting a more radiant and healthiest skin compared to volunteers applying CBD formula. Scientific literature was previously reviewed that establishes CBD activities explaining its growing interest and use in the cosmetic industry: antioxidant, anti-inflammatory, β -endorphin inductor, skin redness reduction, mood enhancer [57]. Finally, in the tested conditions, SM appeared as efficient as CBD to promote CB2R and β -endorphin in mast cells and better improved sensitive skin condition on women exposed to UV and air pollution.

5. Conclusion

This study reports SM protective effects against consequences of combined exposure to UV and air pollution. By reducing oxidative stress and inhibiting pro-inflammatory cytokines SM preserved oxinflammation balance. SM bioactivity appeared being mediated by AHR and Nrf2 signaling. Clinical study confirmed SM to improve urban skins complexion and be an alternative to CBD. As a new finding, SM activated CB2R in mast cells and the release of β -endorphin, opening new lead in the understanding of anti-inflammatory mechanisms of the flavonoid complex.

Author Contributions: Conceptualization, Cloe Boira, Amandine Scandolera and Romain Reynaud; methodology, Cloe Boira, Emilie Chapuis, Amandine Scandolera and Romain Reynaud; validation, Cloe Boira, Emilie Chapuis, Amandine Scandolera, and Romain Reynaud; formal analysis, Cloe Boira and Emilie Chapuis; investigation, Cloe Boira; writing—original draft preparation, Cloe Boira; writing-review and editing, Cloe Boira, Emilie Chapuis, Amandine Scandolera and Romain Reynaud. All authors have read and agreed to the published version of the manuscript.

Funding: This research received no external funding.

Institutional Review Board Statement: The study was conducted in accordance with the Declaration of Helsinki and did not meet the criteria requiring evaluation by an ethics committee.

Informed Consent Statement: Informed consent was obtained from all subjects involved in the study.

Data Availability Statement: Not applicable.

Acknowledgments: We would like to thank SpinControl, Eurofins, QIMA Life Sciences and the University of Wien for their support conducting some experiments. We would also like to acknowledge Carole Chaumienne Lambert for her support in the redaction of this paper.

Conflicts of Interest: The authors declare no conflict of interest.

References

1. Krutmann, J.; Bouloc, A.; Sore, G.; Bernard, B.A.; Passeron, T. The Skin Aging Exposome. *Journal of Dermatological Science* **2017**, *85*, 152–161, doi:10.1016/j.jdermsci.2016.09.015.
2. Rinnerthaler, M.; Bischof, J.; Streubel, M.K.; Trost, A.; Richter, K. Oxidative Stress in Aging Human Skin. *Biomolecules* **2015**, *5*, 545–589, doi:10.3390/biom5020545.
3. Burke, K.E.; Wei, H. Synergistic Damage by UVA Radiation and Pollutants. *Toxicol Ind Health* **2009**, *25*, 219–224, doi:10.1177/0748233709106067.
4. Soeur, J.; Belaïdi, J.-P.; Chollet, C.; Denat, L.; Dimitrov, A.; Jones, C.; Perez, P.; Zanini, M.; Zobiri, O.; Mezzache, S.; et al. Photo-Pollution Stress in Skin: Traces of Pollutants (PAH and Particulate Matter) Impair Redox Homeostasis in Keratinocytes Exposed to UVA1. *J Dermatol Sci* **2017**, *86*, 162–169, doi:10.1016/j.jdermsci.2017.01.007.
5. Ferrara, F.; Woodby, B.; Pecorelli, A.; Schiavone, M.L.; Pambianchi, E.; Messano, N.; Therrien, J.-P.; Choudhary, H.; Valacchi, G. Additive Effect of Combined Pollutants to UV Induced Skin OxInflammation Damage. Evaluating the Protective Topical Application of a Cosmeceutical Mixture Formulation. *Redox Biology* **2020**, *34*, 101481, doi:10.1016/j.redox.2020.101481.
6. Ferrara, F.; Pambianchi, E.; Woodby, B.; Messano, N.; Therrien, J.-P.; Pecorelli, A.; Canella, R.; Valacchi, G. Evaluating the Effect of Ozone in UV Induced Skin Damage. *Toxicology Letters* **2021**, *338*, 40–50, doi:10.1016/j.toxlet.2020.11.023.
7. Ma, Q. Role of Nrf2 in Oxidative Stress and Toxicity. *Annu Rev Pharmacol Toxicol* **2013**, *53*, 401–426, doi:10.1146/annurev-pharmtox-011112-140320.
8. Puri, P.; Nandar, S.K.; Kathuria, S.; Ramesh, V. Effects of Air Pollution on the Skin: A Review. *Indian J Dermatol Venereol Leprol* **2017**, *83*, 415–423, doi:10.4103/0378-6323.199579.
9. Cervellati, F.; Woodby, B.; Benedusi, M.; Ferrara, F.; Guiotto, A.; Valacchi, G. Evaluation of Oxidative Damage and Nrf2 Activation by Combined Pollution Exposure in Lung Epithelial Cells. *Environ Sci Pollut Res Int* **2020**, *27*, 31841–31853, doi:10.1007/s11356-020-09412-w.
10. Papaccio, F.; D'Arino, A.; Caputo, S.; Bellei, B. Focus on the Contribution of Oxidative Stress in Skin Aging. *Antioxidants* **2022**, *11*, 1121, doi:10.3390/antiox11061121.
11. Vermeij, W.P.; Alia, A.; Backendorf, C. ROS Quenching Potential of the Epidermal Cornified Cell Envelope. *J Invest Dermatol* **2011**, *131*, 1435–1441, doi:10.1038/jid.2010.433.
12. Valacchi, G.; Virgili, F.; Cervellati, C.; Pecorelli, A. OxInflammation: From Subclinical Condition to Pathological Biomarker. *Front. Physiol.* **2018**, *9*, 858, doi:10.3389/fphys.2018.00858.
13. Furue, M.; Uchi, H.; Mitoma, C.; Hashimoto-Hachiya, A.; Chiba, T.; Ito, T.; Nakahara, T.; Tsuji, G. Antioxidants for Healthy Skin: The Emerging Role of Aryl Hydrocarbon Receptors and Nuclear Factor-Erythroid 2-Related Factor-2. *Nutrients* **2017**, *9*, 223, doi:10.3390/nu9030223.
14. Parrado, C.; Mercado-Saenz, S.; Perez-Davo, A.; Gilaberte, Y.; Gonzalez, S.; Juarranz, A. Environmental Stressors on Skin Aging. Mechanistic Insights. *Front Pharmacol* **2019**, *10*, 759, doi:10.3389/fphar.2019.00759.
15. Furue, M.; Hashimoto-Hachiya, A.; Tsuji, G. Antioxidative Phytochemicals Accelerate Epidermal Terminal Differentiation via the AHR-OVOL1 Pathway: Implications for Atopic Dermatitis. *Acta Derm Venerol* **2018**, *98*, 918–923, doi:10.2340/00015555-3003.
16. Galán-Ganga, M.; Del Río, R.; Jiménez-Moreno, N.; Díaz-Guerra, M.; Lastres-Becker, I. Cannabinoid CB2 Receptor Modulation by the Transcription Factor NRF2 Is Specific in Microglial Cells. *Cell Mol Neurobiol* **2020**, *40*, 167–177, doi:10.1007/s10571-019-00719-y.
17. Zhang, M.; Zhang, M.; Wang, L.; Yu, T.; Jiang, S.; Jiang, P.; Sun, Y.; Pi, J.; Zhao, R.; Guan, D. Activation of Cannabinoid Type 2 Receptor Protects Skeletal Muscle from Ischemia-Reperfusion Injury Partly via Nrf2 Signaling. *Life Sciences* **2019**, *230*, 55–67, doi:10.1016/j.lfs.2019.05.056.
18. McDonnell, C.; Leánez, S.; Pol, O. The Inhibitory Effects of Cobalt Protoporphyrin IX and Cannabinoid 2 Receptor Agonists in Type 2 Diabetic Mice. *International Journal of Molecular Sciences* **2017**, *18*, 2268, doi:10.3390/ijms18112268.
19. He, Y.; Jia, H.; Yang, Q.; Shan, W.; Chen, X.; Huang, X.; Liu, T.; Sun, R. Specific Activation of CB2R Ameliorates Psoriasis-Like Skin Lesions by Inhibiting Inflammation and Oxidative Stress. *Inflammation* **2023**, *46*, 1255–1271, doi:10.1007/s10753-023-01805-6.
20. Ibrahim, M.M.; Porreca, F.; Lai, J.; Albrecht, P.J.; Rice, F.L.; Khodorova, A.; Davar, G.; Makriyannis, A.; Vanderah, T.W.; Mata, H.P.; et al. CB2 Cannabinoid Receptor Activation Produces Antinociception by

- Stimulating Peripheral Release of Endogenous Opioids. *Proc Natl Acad Sci U S A* **2005**, *102*, 3093–3098, doi:10.1073/pnas.0409888102.
21. Benedusi, M.; Kerob, D.; Guiotto, A.; Cervellati, F.; Ferrara, F.; Pambianchi, E. Topical Application of M89PF Containing Vichy Mineralising Water and Probiotic Fractions Prevents Cutaneous Damage Induced by Exposure to UV and O₃. *Clin Cosmet Investig Dermatol* **2023**, *16*, 1769–1776, doi:10.2147/CCID.S414011.
 22. Vostálová, J.; Tinková, E.; Biedermann, D.; Kosina, P.; Ulrichová, J.; Rajnochová Svobodová, A. Skin Protective Activity of Silymarin and Its Flavonolignans. *Molecules* **2019**, *24*, 1022, doi:10.3390/molecules24061022.
 23. Katiyar, S.K.; Meleth, S.; Sharma, S.D. Silymarin, a Flavonoid from Milk Thistle (*Silybum Marianum* L.), Inhibits UV-Induced Oxidative Stress Through Targeting Infiltrating CD11b+ Cells in Mouse Skin. *Photochem Photobiol* **2008**, *84*, 266–271, doi:10.1111/j.1751-1097.2007.00241.x.
 24. Frankova, J.; Juranova, J.; Biedermann, D.; Ulrichova, J. Influence of Silymarin Components on Keratinocytes and 3D Reconstructed Epidermis. *Toxicol In Vitro* **2021**, *74*, 105162, doi:10.1016/j.tiv.2021.105162.
 25. Surai, P.F. Silymarin as a Natural Antioxidant: An Overview of the Current Evidence and Perspectives. *Antioxidants* **2015**, *4*, 204–247, doi:10.3390/antiox4010204.
 26. Vargas-Mendoza, N.; Morales-González, Á.; Morales-Martínez, M.; Soriano-Ursúa, M.A.; Delgado-Olivares, L.; Sandoval-Gallegos, E.M.; Madrigal-Bujaidar, E.; Álvarez-González, I.; Madrigal-Santillán, E.; Morales-Gonzalez, J.A. Flavolignans from Silymarin as Nrf2 Bioactivators and Their Therapeutic Applications. *Biomedicines* **2020**, *8*, 122, doi:10.3390/biomedicines8050122.
 27. Pouwer, F.; van der Ploeg, H.M.; Adèr, H.J.; Heine, R.J.; Snoek, F.J. The 12-Item Well-Being Questionnaire. An Evaluation of Its Validity and Reliability in Dutch People with Diabetes. *Diabetes Care* **1999**, *22*, 2004–2010, doi:10.2337/diacare.22.12.2004.
 28. Passeron, T.; Krutmann, J.; Andersen, M. I.; Katta, R.; Zouboulis, C. c. Clinical and Biological Impact of the Exposome on the Skin. *Journal of the European Academy of Dermatology and Venereology* **2020**, *34*, 4–25, doi:10.1111/jdv.16614.
 29. Martin, P.; Goldstein, J.D.; Mermoud, L.; Diaz-Barreiro, A.; Palmer, G. IL-1 Family Antagonists in Mouse and Human Skin Inflammation. *Front Immunol* **2021**, *12*, 652846, doi:10.3389/fimmu.2021.652846.
 30. Yang, L.; Fan, X.; Cui, T.; Dang, E.; Wang, G. Nrf2 Promotes Keratinocyte Proliferation in Psoriasis through Up-Regulation of Keratin 6, Keratin 16, and Keratin 17. *J Invest Dermatol* **2017**, *137*, 2168–2176, doi:10.1016/j.jid.2017.05.015.
 31. Houesson, A.; François, C.; Sauzay, C.; Louandre, C.; Mongelard, G.; Godin, C.; Bodeau, S.; Takahashi, S.; Saidak, Z.; Gutierrez, L.; et al. Metallothionein-1 as a Biomarker of Altered Redox Metabolism in Hepatocellular Carcinoma Cells Exposed to Sorafenib. *Molecular Cancer* **2016**, *15*, 38, doi:10.1186/s12943-016-0526-2.
 32. Chung, J.H.; Youn, S.H.; Koh, W.S.; Eun, H.C.; Cho, K.H.; Park, K.C.; Youn, J.I. Ultraviolet B Irradiation-Enhanced Interleukin (IL)-6 Production and mRNA Expression Are Mediated by IL-1 Alpha in Cultured Human Keratinocytes. *J Invest Dermatol* **1996**, *106*, 715–720, doi:10.1111/1523-1747.ep12345608.
 33. Magcwebeba, T.; Riedel, S.; Swanevelder, S.; Bouic, P.; Swart, P.; Gelderblom, W. Interleukin-1a Induction in Human Keratinocytes (HaCaT): An *In Vitro* Model for Chemoprevention in Skin. *Journal of Skin Cancer* **2012**, *2012*, e393681, doi:10.1155/2012/393681.
 34. Costantini, C.; Renga, G.; Oikonomou, V.; Paolicelli, G.; Borghi, M.; Pariano, M.; De Luca, A.; Puccetti, M.; Stincardini, C.; Mosci, P.; et al. The Mast Cell-Aryl Hydrocarbon Receptor Interplay at the Host-Microbe Interface. *Mediators of Inflammation* **2018**, *2018*, 1–6, doi:10.1155/2018/7396136.
 35. Sehra, S.; Serezani, A.P.M.; Ocaña, J.A.; Travers, J.B.; Kaplan, M.H. Mast Cells Regulate Epidermal Barrier Function and the Development of Allergic Skin Inflammation. *Journal of Investigative Dermatology* **2016**, *136*, 1429–1437, doi:10.1016/j.jid.2016.03.019.
 36. Ständer, S.; Schmelz, M.; Metze, D.; Luger, T.; Rukwied, R. Distribution of Cannabinoid Receptor 1 (CB1) and 2 (CB2) on Sensory Nerve Fibers and Adnexal Structures in Human Skin. *Journal of Dermatological Science* **2005**, *38*, 177–188, doi:10.1016/j.jdermsci.2005.01.007.
 37. Casares, L.; García, V.; Garrido-Rodríguez, M.; Millán, E.; Collado, J.A.; García-Martín, A.; Peñarando, J.; Calzado, M.A.; De La Vega, L.; Muñoz, E. Cannabidiol Induces Antioxidant Pathways in Keratinocytes by Targeting BACH1. *Redox Biology* **2020**, *28*, 101321, doi:10.1016/j.redox.2019.101321.

38. Jang, Y. su; Jeong, S.; Kim, A. -ram; Mok, B.R.; Son, S.J.; Ryu, J.; Son, W.S.; Yun, S.K.; Kang, S.; Kim, H.J.; et al. Cannabidiol Mediates Epidermal Terminal Differentiation and Redox Homeostasis through Aryl Hydrocarbon Receptor (AhR)-Dependent Signaling. *Journal of Dermatological Science* **2023**, *109*, 61–70, doi:10.1016/j.jdermsci.2023.01.008.
39. Baswan, S.M.; Klosner, A.E.; Glynn, K.; Rajgopal, A.; Malik, K.; Yim, S.; Stern, N. Therapeutic Potential of Cannabidiol (CBD) for Skin Health and Disorders. *Clin Cosmet Investig Dermatol* **2020**, *13*, 927–942, doi:10.2147/CCID.S286411.
40. Marrot, L. Pollution and Sun Exposure: A Deleterious Synergy. Mechanisms and Opportunities for Skin Protection. *Curr Med Chem* **2018**, *25*, 5469–5486, doi:10.2174/0929867324666170918123907.
41. Li, Y.-R.; Li, G.-H.; Zhou, M.-X.; Xiang, L.; Ren, D.-M.; Lou, H.-X.; Wang, X.-N.; Shen, T. Discovery of Natural Flavonoids as Activators of Nrf2-Mediated Defense System: Structure-Activity Relationship and Inhibition of Intracellular Oxidative Insults. *Bioorganic & Medicinal Chemistry* **2018**, *26*, 5140–5150, doi:10.1016/j.bmc.2018.09.010.
42. Khan, H.; Tundis, R.; Ullah, H.; Aschner, M.; Belwal, T.; Mirzaei, H.; Akkol, E.K. Flavonoids Targeting NRF2 in Neurodegenerative Disorders. *Food and Chemical Toxicology* **2020**, *146*, 111817, doi:10.1016/j.fct.2020.111817.
43. Mendonca, P.; Soliman, K.F.A. Flavonoids Activation of the Transcription Factor Nrf2 as a Hypothesis Approach for the Prevention and Modulation of SARS-CoV-2 Infection Severity. *Antioxidants* **2020**, *9*, 659, doi:10.3390/antiox9080659.
44. L Suraweera, T.; Rupasinghe, H.P.V.; Dellaire, G.; Xu, Z. Regulation of Nrf2/ARE Pathway by Dietary Flavonoids: A Friend or Foe for Cancer Management? *Antioxidants (Basel)* **2020**, *9*, 973, doi:10.3390/antiox9100973.
45. Furue, M. Regulation of Filaggrin, Loricrin, and Involucrin by IL-4, IL-13, IL-17A, IL-22, AHR, and NRF2: Pathogenic Implications in Atopic Dermatitis. *International Journal of Molecular Sciences* **2020**, *21*, 5382, doi:10.3390/ijms21155382.
46. Lessard, J.C.; Piña-Paz, S.; Rotty, J.D.; Hickerson, R.P.; Kaspar, R.L.; Balmain, A.; Coulombe, P.A. Keratin 16 Regulates Innate Immunity in Response to Epidermal Barrier Breach. *Proceedings of the National Academy of Sciences* **2013**, *110*, 19537–19542, doi:10.1073/pnas.1309576110.
47. Edamitsu, T.; Taguchi, K.; Okuyama, R.; Yamamoto, M. AHR and NRF2 in Skin Homeostasis and Atopic Dermatitis. *Antioxidants* **2022**, *11*, 227, doi:10.3390/antiox11020227.
48. Wu, Q.; Ma, Y.; Liu, Y.; Wang, N.; Zhao, X.; Wen, D. CB2R Agonist JWH-133 Attenuates Chronic Inflammation by Restraining M1 Macrophage Polarization via Nrf2/HO-1 Pathway in Diet-Induced Obese Mice. *Life Sci* **2020**, *260*, 118424, doi:10.1016/j.lfs.2020.118424.
49. Li, L.; Liu, X.; Ge, W.; Chen, C.; Huang, Y.; Jin, Z.; Zhan, M.; Duan, X.; Liu, X.; Kong, Y.; et al. CB2R Deficiency Exacerbates Imiquimod-Induced Psoriasiform Dermatitis and Itch Through the Neuro-Immune Pathway. *Front Pharmacol* **2022**, *13*, 790712, doi:10.3389/fphar.2022.790712.
50. Du, Y.; Ren, P.; Wang, Q.; Jiang, S.-K.; Zhang, M.; Li, J.-Y.; Wang, L.-L.; Guan, D.-W. Cannabinoid 2 Receptor Attenuates Inflammation during Skin Wound Healing by Inhibiting M1 Macrophages Rather than Activating M2 Macrophages. *J Inflamm* **2018**, *15*, 25, doi:10.1186/s12950-018-0201-z.
51. Atalay, S.; Jarocka-Karpowicz, I.; Skrzydlewska, E. Antioxidative and Anti-Inflammatory Properties of Cannabidiol. *Antioxidants* **2020**, *9*, 21, doi:10.3390/antiox9010021.
52. Jarocka-Karpowicz, I.; Biernacki, M.; Wroński, A.; Gęgotek, A.; Skrzydlewska, E. Cannabidiol Effects on Phospholipid Metabolism in Keratinocytes from Patients with Psoriasis Vulgaris. *Biomolecules* **2020**, *10*, 367, doi:10.3390/biom10030367.
53. Gęgotek, A.; Atalay, S.; Domingues, P.; Skrzydlewska, E. The Differences in the Proteome Profile of Cannabidiol-Treated Skin Fibroblasts Following UVA or UVB Irradiation in 2D and 3D Cell Cultures. *Cells* **2019**, *8*, 995, doi:10.3390/cells8090995.
54. Bíró, T.; Tóth, B.I.; Haskó, G.; Paus, R.; Pacher, P. The Endocannabinoid System of the Skin in Health and Disease: Novel Perspectives and Therapeutic Opportunities. *Trends in Pharmacological Sciences* **2009**, *30*, 411–420, doi:10.1016/j.tips.2009.05.004.
55. Fink, B.; Matts, P.J.; D'Emiliano, D.; Bunse, L.; Weege, B.; Röder, S. Colour Homogeneity and Visual Perception of Age, Health and Attractiveness of Male Facial Skin. *J Eur Acad Dermatol Venereol* **2012**, *26*, 1486–1492, doi:10.1111/j.1468-3083.2011.04316.x.

56. Sun, Y.-H.P.; Zhang, X.; Lu, N.; Li, J.; Wang, Z. Your Face Looks the Same as before, Only Prettier: The Facial Skin Homogeneity Effects on Face Change Detection and Facial Attractiveness Perception. *Front Psychol* **2022**, *13*, 935347, doi:10.3389/fpsyg.2022.935347.
57. Melas, P.A.; Scherma, M.; Fratta, W.; Cifani, C.; Fadda, P. Cannabidiol as a Potential Treatment for Anxiety and Mood Disorders: Molecular Targets and Epigenetic Insights from Preclinical Research. *Int J Mol Sci* **2021**, *22*, 1863, doi:10.3390/ijms22041863.

Disclaimer/Publisher's Note: The statements, opinions and data contained in all publications are solely those of the individual author(s) and contributor(s) and not of MDPI and/or the editor(s). MDPI and/or the editor(s) disclaim responsibility for any injury to people or property resulting from any ideas, methods, instructions or products referred to in the content.